

Influence of fibre-surface treatment on structural, thermal and mechanical properties of jute

E. Sinha · S. K. Rout

Received: 23 November 2007 / Accepted: 15 January 2008 / Published online: 20 February 2008
© Springer Science+Business Media, LLC 2008

Abstract Jute fibres, an environmentally and ecologically friendly product, were chemically modified by treatment with 1.26 M (5 wt%) solution of NaOH solution at room temperature for 2, 4 and 8 h. The above samples were characterized by small angle X-ray scattering (SAXS) technique and XRD for macromolecular and microstructural parameters of fibres before and after alkali treatment where as FT-IR and SEM was used for fine structural details and morphological studies of the fibres. Differential scanning calorimetry (DSC) and instron 1185 analyzed thermal and mechanical behaviour of the fibres. Comparison and analysis of results confirmed some changes in the macromolecular structure and microstructure of the fibres after chemical treatment due to swelling of macromolecules and removal of some non-crystalline constituents of the fibres. The findings conclude that change in crystallinity developed after alkali treatment resulting improvement in mechanical strength of the fibres. However, the removal of structural constituents after alkali treatment leads the thermal decomposition temperature of the cellulose went down to 360.62 °C after 8 h alkali treatment from 365.26 °C for raw jute fibre.

Introduction

During the past decade, increasing environmental awareness, new global agreements and international governmental policies and regulations have been the driving force behind the renewed interest in the natural fibres. The attractiveness of a plant-based fibre comes from its high-specific strength and stiffness, natural availability and environmental 'friendliness'. Natural cellulose-based fibres are gaining increasing attention for their diversified applications in engineering and their uses, such as building materials and structural parts for the automotive application, where lightweight is required. The approximate chemical composition of the jute fibre [1] in wt.% is: cellulose (58–63), hemicelluloses (20–22), lignin (12–15), small amounts of protein (2%), mineral matter (1%) and trace quantities of organic and inorganic pigments. The elementary units of cellulose macromolecules are anhydro-D-glucose which contains three hydroxyls (–OH) [1]. These hydroxyls form the hydrogen bonds inside the macromolecule itself (intramolecular) and between the other cellulose macromolecules (intermolecular) as well. Therefore, all vegetable fibres are hydrophilic in nature, and their moisture contents lies between 3 and 13% [2], which is one of the reasons for the degradation of the fibres. Although, as with most of the other plant-based natural fibres, cellulose forms the main structural components, lignin and hemicelluloses also play an important part in determining the characteristic properties of the fibres. Jute hemicelluloses, which are thought to consist principally of xylan, polyuronide and hexosan have been shown to be very sensitive to the action of caustic soda, which also exerts some effects on lignin and α -cellulose [3]. Several authors have employed the technique of mercerization for jute and the changes occurring in the fibre properties have been

E. Sinha (✉)
Department of Physics, National Institute of Technology,
Rourkela, Orissa 769008, India
e-mail: elasinha@rediffmail.com

S. K. Rout
Department of Applied Physics, Birla Institute of Technology,
Mesra, Ranchi, Jharkhand, India
e-mail: skrout@bitmesra.ac.in

investigated. Sarkar [4] treated jute fibres with NaOH solution of concentration 1 and 8% for 48 h and observed 130% improvement in the tensile strength of the fibres in both the cases. Similarly, jute fibres were treated with 2% NaOH solution for 1 h by Samal et al. [5] and 13% improvement in the tenacity of the fibres was reported. Prasad et al. [6] observed that coir fibre when alkali treated at 5% NaOH for 72–96 h showed improvement in tensile strength by 10–15%, modulus by 40%. Rout et al. [7] reported improvement of 35% in tensile strength, 60% in flexural strength and 69% in impact strength of the composites containing 5% alkali treated reinforced natural fibres.

As jute fibres are cellulosic in nature and are comprised of macromolecules, the small-angle X-ray scattering has been undertaken to analyze some macromolecular structure. To be specific the SAXS is due to the heterogeneity of electron densities occurring in matter at colloidal dimension [8, 9]. There will be no scattering if density is uniform. For the sake of demonstration, the system is considered as the two-phase system (i.e., cellulose and void) and the square of their density differences $(\Delta\rho)^2$ takes about hundred times the value of that between crystalline and amorphous cellulose [10]. Hence we treat jute fibre as the system and the cellulose and void as the two phases. The electron density difference between the two phases of the system, which occurs over a distance of 10–100 nm, causes the small angle X-ray scattering. This phenomenon was first observed by many researchers [11–13]. Porod's laws [14, 15] were applied to obtain physical parameters of densely packed system for an ideal two-phase structure having sharply defined phase boundaries. Latter, Vonk [16] explained that always the electron density does not change abruptly, but changes gradually over the certain range between two phases. This range is called the width of the transition layer E . Such a system is known as a non-ideal, two-phase system. This model of non-ideal, two-phase system can be considered as one in which the hard core is coated with a soft sheath with a continuously varying electron density.

In the present investigation, an effort was made to study some mechanical and thermal behaviour of the raw (dewaxed) and 1.26 M (5 wt%) solution of NaOH treated jute fibres for 2, 4 and 8 h, and it was tried to correlate this behaviour with their macromolecular structure analyzed by small-angle X-ray scattering (SAXS) at room temperature. Crystallinity and surface morphology was investigated by XRD and SEM methods. FT-IR spectra were recorded to study the fine structural characteristics of cellulose, hemicelluloses and lignin as per [17]. Thermal property and mechanical properties of fibres were analyzed by DSC and Instron 1185.

Experimental details and core mathematics

Materials

Jute fibres (*Corchorus olitorous*) were collected from Central Research Institute for Jute and Allied Fibre Technology (CRIJAF), Kolkata.

Methods

Dewaxing

Collected fibres were dewaxed in a (1:2) mixture of alcohol and benzene as done by Roy [18]. As a result of this treatment, the specimen attains a “hohlraum” character (according to Porod [19] and Ratho et al. [20]), i.e., the substance occurs in layers like the pages of a book with free space in between. This is treated as a raw sample in this study.

Surface treatment

The jute fibres were cut to 500 mm of length and were soaked in a 1.26 M solution of NaOH solution at 30 °C for 2, 4 and 8 h. The fibres were then washed several times with distilled water to remove any NaOH sticking to the fibre surface, neutralized with dilute acetic acid and washed again with distilled water. Final pH maintained was 7.0. The fibres were then dried at room temperature for 48 h, followed by oven drying at 100 °C for 6 h for the removal of moisture content. The 1.26 M solution of NaOH treated fibres for 2, 4 and 8 h are regarded as M jute 2 h, M jute 4 h and M jute 8 h, respectively, hereafter. M stands for mercerization because alkali treatment is also known as mercerization.

Fibre testing

The weight changes of the fibres after different soaking time in 1.26 M solution of NaOH were determined by % weight loss calculated as:

$$\% \text{Weight loss} = (W_1 - W_2) \times 100 / W_1$$

where W_1 was the weight of fixed amount of dry raw jute fibres whereas W_2 was the weight of dry fibres after being treated with alkali solution. Fibre fineness was determined in terms of linear density in accordance with ASTM D1577-92. The linear density was calculated on the basis of the weight of 100 single fibres of 60 mm length each and converted into tex. The major constituents (α -cellulose,

hemicelluloses and lignin) of the raw and alkali-treated jute fibre samples were determined by chemical analysis as per the standard procedure [21].

Scanning Electron Microscopy study

The scanning electron micrographs of the samples were taken in Hitachi (S-3400N) SEM. The samples were coated with a 20-nm thick gold layer.

Fourier Transform Infrared Spectroscopy (FT-IR)

The raw and alkali-treated jute fibres were analyzed by FT-IR spectroscopy. Room-temperature FT-IR spectra were recorded on solid samples in KBr pellets by means of a Shimadzu FT-IR spectrometer (IRPrestige-21) with a resolution of 4 cm^{-1} . The spectra were smoothened with constant smooth factor for comparison.

Small angle X-ray scattering (SAXS)

X-ray measurement and computational analysis. Room-temperature, smeared-out, small-angle X-ray scattering data for jute fibres were collected from a line collimated SAXS camera (Anton Park, Austria). The Cu- K_α lines were used as incident radiation from PANalítica X-ray source (PW3830) at 40 kV (40 mA) operating voltage. The sample to detector distance “ a ” was 26.45 cm. The scattering intensities were collected in a two-dimensional, position sensitive image plate (Packard Bioscience Inc.). To have digitized data, the image plate was scanned in a cyclone storage phosphor scanner (Perkin Elmer) with the help of the supplied computer program “Optiquant”. The observed two-dimensional intensities were integrated over a line profile to convert into one-dimensional scattering data with the help of the supplied computer program “SAXS quant”. All the computational works were performed using a self-developed program written in MATLAB 6.5. The program comprises the computation of the relevant parameters by SAXS including one- and three-dimensional correlation functions. The reliability of the program was checked with the experimental data and results for sisal fibre, available with the author.

Theory. It has been shown by Vonk [16] that, for a general two-phase system having isotropic structure, the relation

$$16\pi^3 \int_0^\infty S^4 I_a(s) ds = \int_0^\infty |\text{grad}\eta|^2 dV_r \quad (1)$$

holds good, where $I_a(s)$ is the desmeared intensity in the absolute unit, η is the deviation of the electron density of

the sample at any point from the mean value and s is the co-ordinate in the reciprocal or Fourier space given by the relation $s = 2\theta/\lambda$, where 2θ , the scattering angle, is equal to x/a . Here x is the position coordinate of the scattered intensity from the centre of the primary beam. The above equation can be regarded as parallel to the well-known relation

$$4\pi \int_0^\infty S^2 I_a(s) ds = \int_0^\infty \eta^2 dV_r \quad (2)$$

where $\int_0^\infty S^2 I_a(s) ds$ is generally known as the invariant.

If absolute intensities are not available, a very useful parameter R , given by the ratio of Eqs. (1) and (2) can be obtained as

$$\begin{aligned} R &= \frac{|\text{grad}\eta|^2}{\eta^2} = 4\pi^2 \int_0^\infty S^4 I_a(s) ds / \int_0^\infty S^2 I_a(s) ds \\ &= 6\pi^2 \int_0^\infty S^3 \tilde{I}(s) ds / \int_0^\infty S \tilde{I}(s) ds \end{aligned} \quad (3)$$

Here $I_a(s)$ and $\tilde{I}(s)$ are the desmeared and smeared-out intensities, respectively, in arbitrary units.

The ratio R is a useful parameter for the characterization of the structure. In any ideal two-phase structure, the gradient at the phase boundary is infinite and consequently R also goes to infinity. On the other hand, if R is finite, the electron density changes from one phase to the other continuously over a region known as the transition layer of width or thickness E . The above equation has been transformed to variable x by Misra et al. [22] as

$$\begin{aligned} R &= (3/2)(2\pi/\lambda a)^2 \int x^3 \tilde{I}(x) dx / \int x \tilde{I}(x) dx \\ &= (3/2)K^2 A_3/A_1 \end{aligned} \quad (4)$$

The value of R obtained from Eq. 4 determines the nature of the sample, as to whether it belongs to an ideal or non-ideal two-phase system.

In case of non-ideal two-phase system, the important parameter is width of the transition layer, E . The value of E can be obtained from $C(r)$, the three-dimensional correlation function of a sample, normalized to unity at the origin, in real space. The equation connecting E and $C(r)$ has been given by Vonk [16] as

$$E_v = -4/R_1 (dC(r)/dr)_{r=E_v} \quad (5)$$

In order to obtain E , it is required to evaluate the value of $C(r)$ at various values of r in real space. It has been shown by Mering and Tchoubar [23] that $C(r)$ can be calculated from the expression

$$C(r) = \int_0^\infty S \tilde{I}(s) J_0(2\pi r s) ds / \int_0^\infty S \tilde{I}(s) ds \quad (6)$$

where J_0 is the Bessel function of the zero-order and first kind. In the above expression, the three-dimensional

correlation function $C(r)$ is determined from the smeared-out intensity $\tilde{I}(s)$, where the slit correction for infinite height given by the relation, $\tilde{I} = \int_{-\infty}^{\infty} I(\sqrt{s^2 + t^2}) dt$ is incorporated [24] and contained in the Bessel function J_0 . Here ‘ t ’ is the arbitrary variable representing the slit height and $C(r)$ has been written in terms of x by Misra et al. [22] as

$$C(r) = \int_0^\infty x \tilde{I}(x) J_0\left(\frac{2\pi r x}{\lambda a}\right) dx / \int_0^\infty x \tilde{I}(x) dx \tag{7}$$

For a layer structure, Kortleve and Vonk [25] have used the one-dimensional correlation function $C_1(y)$. Mering and Tchoubar [23] have shown that

$$C_1(y) = \int_0^\infty s \tilde{I}(s) [J_0(Z) - Z J_1(Z)] ds / \int_0^\infty s \tilde{I}(s) ds \tag{8}$$

Here $Z = 2\pi s y$ and J_1 is the Bessel function of the first order, first kind. When changed to the x variable, the above equation [22] reduces to

$$C_1(y) = \int_0^\infty x \tilde{I}(x) [J_0(Z) - Z J_1(Z)] dx / \int_0^\infty x \tilde{I}(x) dx \tag{9}$$

where $Z = 2\pi s y / \lambda a$. It was shown by Vonk [16] that the position of the very first maximum in the one-dimensional correlation function gives the values of average periodicity transverse to the layers, D . The value of D can be obtained by picking up the position of the first subsidiary maximum in $C_1(y)$ versus y curve.

The equation:

$$(dC_1(y)/dy)_{y > E_v} = -1(\Delta\eta)^2 / D \langle \eta^2 \rangle \tag{10}$$

derived by Vonk [16] can be used to calculate the value of $(\Delta\eta)^2 / \langle \eta^2 \rangle$, where $(\Delta\eta)$ is the electron density difference between the two phases. Here, the slope is taken at a point where y is greater than E_v . It has been also proved by Vonk [16] that the second differentials of $C(r)$ and $C_1(y)$ at the origin are given by the relation

$$(d^2C_1(y)/dy^2)_{y=0} = 3(d^2C(r)/dr^2)_{r=0} \tag{11}$$

For a layer structure, as shown by Vonk [16], the specific inner surface, S/V , defined as the phase boundary per unit volume of the dispersed phase, can be written as

$$S/V = 2/D \tag{12}$$

For a non-ideal, two-phase structure, the following relation holds good [16]:

$$\langle \eta^2 \rangle / (\Delta\eta)^2 = \phi_1 \phi_2 - (ES/6V) \tag{13}$$

where ϕ_1 and ϕ_2 are the volume fractions of the matter and void region, respectively. For this, the phase boundary is shown at the middle of the transition layer. Assuming the sum of the volume fraction of both phases to be unity the

values of ϕ_1 and ϕ_2 can be determined from the above relation.

For the two-phase structure, an idea of the statistical distribution of crystalline (matter) and void regions can be formed by shooting arrows in all the possible directions. The average length of the arrow in the two phases are called the transversal lengths \bar{l}_1 and \bar{l}_2 . They are given by Mittelbach and Porod [26] as

$$\bar{l}_1 = 4\phi_1 V/S \quad \text{and} \quad \bar{l}_2 = 4\phi_2 V/S \tag{14}$$

with the range of inhomogeneity \bar{l}_r as

$$1/\bar{l}_r = 1/\bar{l}_1 + 1/\bar{l}_2 \tag{15}$$

The length of the coherence for a specimen, as given by above workers is

$$l_c = 2 \int_0^\infty C(r) dr \tag{16}$$

The value of E can also be calculated by the Ruland method [27] from the plot of $\tilde{I}(x)X$ vs. X^{-2} , known as Ruland plot. The functional relationship of $\tilde{I}(s)$ with s at the tail end of the SAXS pattern, for non-ideal, two-phase system, is given by

$$\tilde{I}(s \rightarrow \infty) = \pi c / 2(1/s^3 - 2\pi^2 E^2 / 3s) \tag{17}$$

Here c is the proportionality constant. For an ideal two-phase structure, $E = 0$ and hence the above equation reduces to Porod’s law. The above equation, when transformed to x , takes the form

$$\tilde{I}(x \rightarrow \infty) \cdot x = \pi c / 2(x^{-2} - \pi^3 c / 3(\lambda a)) E^2 \tag{18}$$

The value of E can be calculated from the graph of $\tilde{I}(s \rightarrow \infty) \cdot x$ vs. x^{-2} , known as Ruland plot.

Background correction. In no experimental set-up it is possible to record the SAXS pattern of the sample alone. A continuous background scattering is always mixed with the SAXS pattern of the experimental sample. It is, therefore, essential to apply the background correction to estimate the effect of continuous background scattering. Therefore special care must be taken to separate the SAXS intensity $\tilde{I}(s)$ from the continuous background scattering $\tilde{I}_{bg}(s)$ [16].

X-ray diffraction

Principle. The strains developed in the crystallites due to chemical treatment manifest as change in lattice planes, causing line shifting. These changes in the lattice planes are measured by X-ray diffraction method. Microstress causes diffraction line broadening, while macrostress causes line shifting. The relation between the broadening produced and the nonuniformity of the strain can be given by the formula $b = \Delta 2\theta = -2\Delta d \tan \theta / d$ derived by

differentiating the Bragg law. Here b is the extra broadening, over and above the instrumental breadth of the line due to a fractional variation in plane spacing $\Delta d/d$ to be calculated from the observed broadening.

If d_i indicates the untreated (unstressed) spacing and d_s the spacing in the treated (strained) fibre, the microstrain in the particles in the direction normal to the diffracting plane is

$$\varepsilon = \Delta d/d = (d_s - d_u/d_u) \quad (19)$$

If $d_s > d_u$, then $\Delta d/d$ is positive which indicates that the residual stress is tensile and if $d_s < d_u$, then $\Delta d/d$ is negative indicating generation of residual compressive stress in the surface. This value of $\Delta d/d$, however, includes both tensile and compressive strains. Assuming both are equal for micro-crystallites, the value of $\Delta d/d$ must be divided by two to obtain the maximum tensile strain alone, or maximum compressive strain alone [28]. Again, maximum microstress present in the sample can be defined as

$$\sigma_{\text{stress}} = \varepsilon E/2 \quad (20)$$

Putting the value of the ε , we obtain

$$\sigma_{\text{stress}} = \Delta d E/2d \quad (21)$$

where E is the elastic constant or generally known as Young's modulus of the material.

The crystallite size of the samples was calculated using well-known Scherrer formula [29]. The crystallinity index (CrI) of the fibres was calculated according to the Segal empirical method as follows [30].

Experimental techniques. The X-ray diffraction data were collected using a Philips Analytical X-ray Instrument, X'Pert-MPD (PW 3020 vertical goniometer and 3710 MPD control unit) employing Bragg-Brentano parafocusing optics. The XRD patterns were recorded with a step size of 0.01° on a $5\text{--}50^\circ$ range with a scanning rate of 2° per min. Line focus Ni-filtered CuK_α radiation from an X-ray tube (operated at 40 kV and 30 mA) was collimated through soller slit (SS) of 0.04 rad., fixed divergence slit of 1° and mask (5 mm) before getting it diffracted from the sample. Experimental control and data acquisition were full automated through computer.

Mechanical properties analysis

Tensile tests of single jute fibres were carried out using an Instron 1185 at National Institute of Research on Jute and Allied Fibre Technology (NIRJAFT), Kolkata. A gauge length of 10 mm was employed with a cross-head speed of 5 mm/min. A total of 50 fibres of both treated and untreated samples having length 50 mm with magnification 50:1 were tested and the mean values were considered.

Thermal analysis

DSC measurements were performed using a (TA Instrument, USA, Model no. Q 10) thermal analyzer. A heating rate of $10^\circ\text{C}/\text{min}$ and a sample weight of 3–4 mg in an aluminium crucible with a pin hole were used in a nitrogen atmosphere ($50\text{ mL}/\text{min}$).

Results and discussion

Chemical analysis

Figure 1 shows the weight loss of the fibre and its major constituents with the alkali treatment time. The weight of the fibres was found to be decreasing after each alkali treatments. The content of hemicelluloses and lignin gradually decreased with treatment hours but the content of α -cellulose remained almost constant before and after alkali treatment of the jute fibre. Similar observations are also reported by Ray et al. [31] in case of another species of jute fibre, *Corchorus capsularies*.

Surface morphology by SEM

The surface morphology of raw and mercerized jute fibres was analyzed by scanning electron microscope (SEM). The SEM pictures of both raw and mercerized surfaces are shown in Fig. 2. The surfaces of raw jute were found to be smooth and showed their multicellular nature, whereas rough surface morphology and fragments on the surface of the mercerized jute fibre were observed (Fig. 2). It is also found that roughness increases as the treating time increases. The rough surface morphology was typical for the treated fibres, because of the removal of lignin and

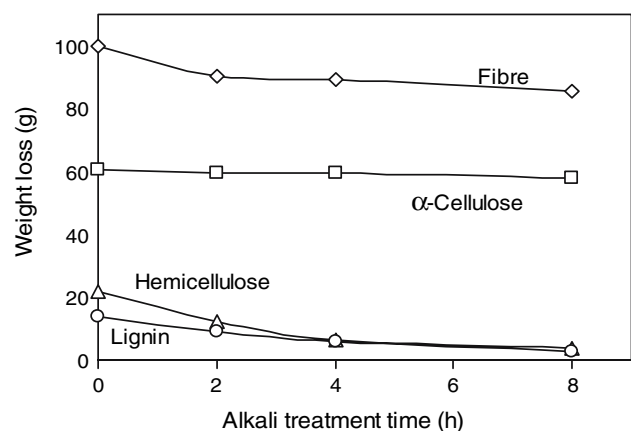
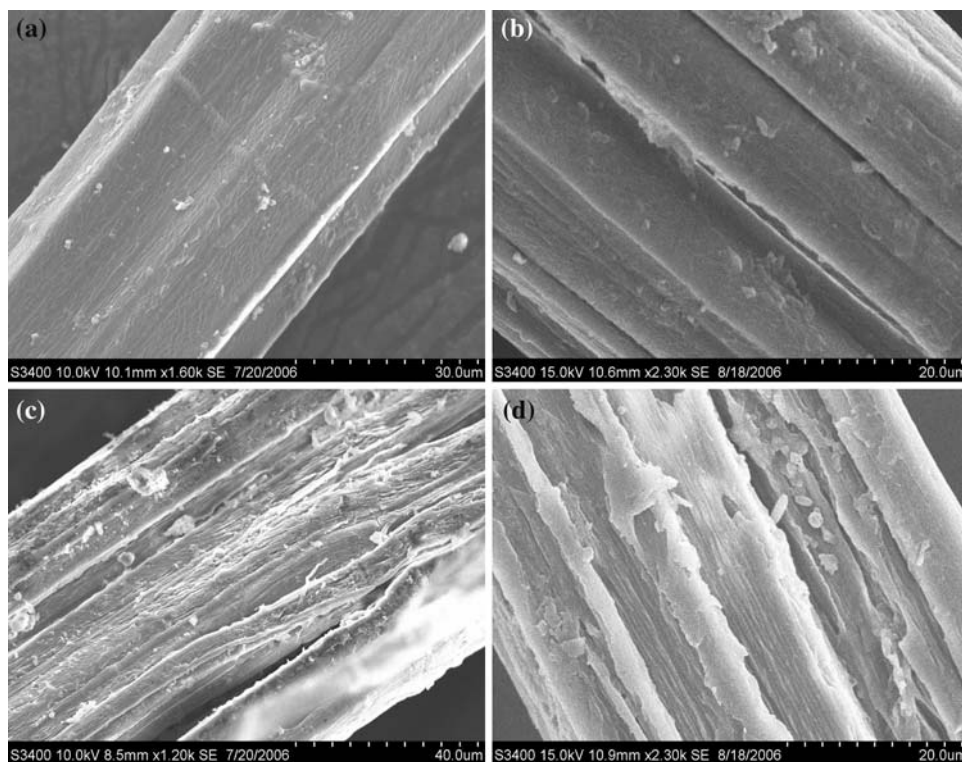


Fig. 1 Loss of the weight of the constituents of the jute fibres after alkali treatment

Fig. 2 Surface morphology of different jute fibres: (a) raw jute, (b) M jute 2 h, (c) M jute 4 h and (d) M jute 8 h



hemicelluloses and other structural effects [32]. Thus, alkali treatments results in significant change of morphology of the fibre surface and is effective for increasing available contact between fibre and polymatrix.

FT-IR study

IR spectra of the raw and the alkali-treated jute are shown in Fig. 3 from wave number 4000 to 450 cm^{-1} . The characteristic features of the spectrum of the jute are due to its constituents lignin, hemicelluloses and α -cellulose [33].

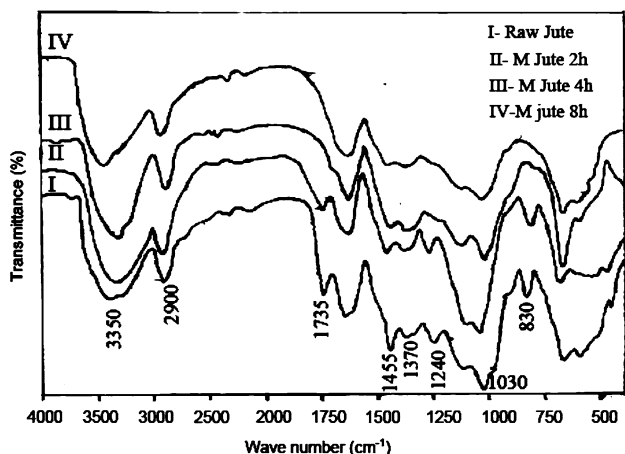


Fig. 3 Infrared spectra of raw and alkali-treated jute fibres

The 2900 cm^{-1} band has been chosen as an internal standard, as it is present as a prominent peak in the IR spectra of raw and alkali-treated jute fibres. This internal standard, though not fully established, has been adopted for making a comparative study of the spectra. The summary of the results, including the significance of the bands, the ratios of absorbance maxima of individual bands, and the 2900 cm^{-1} band (A_v/A_{2900}) are recorded in Table 1.

The 3350 cm^{-1} band, ascribed to H-bonded H–O stretching [34], had almost the same absorbance intensity ratio for the alkali-treated jute samples and raw jute fibre. This finding is in concurrence with the almost constant α -cellulose contents even after mercerization of the jute fibres, as shown in Table 1. The 2900 cm^{-1} is assigned to C–H stretching in methyl and methylene groups [34]. The band near 1735 cm^{-1} which is assigned to the C–O stretching of the carboxyl and acetyl groups in hemicelluloses of the jute fibre [35], was prominent in raw jute fibre. This was found weak after 2 h and absent after 4 h alkali treatment, as shown in Table 1. This can be explained on the basis of removal of hemicelluloses after alkali treatment, which is mainly due to the removal of acetyl group present in hemicelluloses after alkali treatment [36]. The absorbance at 1455 cm^{-1} is attributed to CH_3 deformation (asymmetric) in lignin. The absorption intensity ratios were found to decrease after alkali treatment of jute fibre. This may be due to the loss of lignin after alkali treatment. The band 1370 cm^{-1} , which is ascribed to the C–H deforming (symmetric), may be attributed to lignin, α -cellulose, or

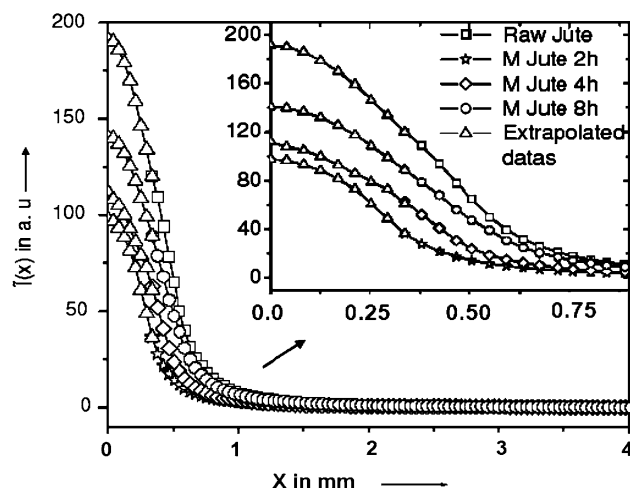
Table 1 Absorbance intensity ratio of IR spectra of raw and alkali-treated jute fibre

| Position of bands (cm^{-1}) | Assignment | Raw Jute (A_{1735}/A_{2900}) | M Jute 2 h (A_{1735}/A_{2900}) | M Jute 4 h (A_{1735}/A_{2900}) | M Jute 8 h (A_{1735}/A_{2900}) |
|--|--|-------------------------------------|---------------------------------------|---------------------------------------|---------------------------------------|
| 3350 | H–O stretching (H bonded) | 1.07 | 1.07 | 1.068 | 1.066 |
| 2900 | C–H stretching in methyl and methylene | 1.0 (0.11) | 1.0 (0.158) | 1.0 (0.073) | 1.0 (0.114) |
| 1735 | C–O stretching in carbonyl and un-conjugated β -ketone | 1.023 | 0.548 | Nil | Nil |
| 1455 | C–H deformation and CH_2 bending | 1.09 | 0.92 | 0.75 | Shoulder |
| 1370 | C–H deforming (asymmetric) | 1.093 | 0.987 | Nil | Nil |
| 1230–1240 | C–O stretching in acetyl group | 1.102 | 0.993 | Nil | Nil |
| 1030 | Aromatic C–H in plane deformation | 1.45 | 1.4 | 1.3 | 1.28 |
| 830 | Aromatic C–H out-of-plane vibration | 0.2 | 0.151 | Shoulder | Shoulder |

xylan, were found with higher absorption ratio for raw jute in comparison to the alkali-treated jute. The medium band at 1240 cm^{-1} , ascribed to C–O stretching in the acetyl in xylan, was found prominent in raw jute, but decreases with alkali treatment due to the removal of acetyl group present in the hemicelluloses. The band 1030 cm^{-1} , which is assigned to aromatic C–H in plane deformation and C–O deformation for primary alcohol in lignin, was found with higher absorption intensity ratio in raw jute compared to alkali-treated fibre. This observation may be ascribed to the loss of lignin from the fibre after alkali treatment. The 830 cm^{-1} , band which is assigned to the aromatic C–H out of phase vibration in lignin was found with higher absorbance intensity for raw jute fibre as compared to the alkali-treated jute.

Macromolecular structure of fibres

The experimental SAXS patterns for raw and alkali-treated jute fibre at room temperature attain a minimum and stable value at $x \geq 4 \text{ mm}$. Hence the intensity at $x = 4 \text{ mm}$ is treated as background scattering intensity, subtracted from the observed intensity and plotted in Fig. 4. The background-corrected SAXS intensities were used for subsequent calculation and plots. At the outset, five background corrected intensity values near the origin were fitted to Gauss curve [37] $\tilde{I}(s \rightarrow 0) = p \exp(-qx^2)$ by least square technique. The values of the constants p and q were obtained as 191.4 and 419.9 for raw jute, whereas 97.7 and 621.5 for 2 h alkali-treated jute, 103.5 and 518.1 for 4 h treatment and 140.8 and 403.0 for 8 h alkali-treated jute, respectively. Taking the values of p and q , the scattering curves for all the cases were extrapolated to $x = 0$. Each extrapolated point is indicated by the symbol “ Δ ”, as shown in Fig. 4. The method of the extrapolation has little effect on the relevant part of the correlation function; neither the position nor the height of the first maximum of

**Fig. 4** Background-corrected, smeared-out scattering curve for different jute fibres

the one-dimensional correlation function is affected. The two integrals in Eq. 4 were calculated by the numerical integration using Trapezoidal rule and the value of R was found to be positive for all the samples, as tabulated in Table 2. The small but positive value of R indicates that the electron density gradient at the phase boundary is finite, suggesting the sample to be a non-ideal, two-phase system [37]. After proper background correction, to have a clear idea on the samples, double logarithmic plot was employed, and is shown in Fig. 5. The slope of the each plot is given in the bracket of the legend for each sample. In all the samples, the slope is greater than -4 , indicating that the samples are of non-ideal, two-phase system [38].

For the various values of r and y , the three and one-dimensional correlation function for the samples were computed, respectively, and are shown in Figs. 6 and 7. It is reported [39] that the cellulose fibrils in jute fibre and in leafy fibres like sisal are arranged in layers. That is why one-dimensional correlation functions is applied and calculated for all the samples of the jute fibres. According to

Table 2 The various physical parameters of the raw and alkali-treated jute fibre derived from SAXS study

| Samples parameters (unit) | Raw jute | M jute 2 h | M jute 4 h | M jute 8 h |
|--|----------|------------|------------|------------|
| R (10^{-2} nm^{-2}) | 3.0542 | 4.8648 | 4.7496 | 4.6046 |
| D (nm) | 85.0 | 114.0 | 100.0 | 86.0 |
| S/V ($\times 10^{-2} \text{ nm}^{-1}$) | 2.35 | 1.75 | 2.0 | 2.30 |
| E_v (nm) | 4.75 | 4.0 | 4.05 | 4.20 |
| E_R (nm) | 4.55 | 3.84 | 3.85 | 3.91 |
| ϕ_1 (%) | 0.806 | 0.896 | 0.88 | 0.85 |
| ϕ_2 (%) | 0.194 | 0.104 | 0.12 | 0.15 |
| \bar{l}_1 (nm) | 137.11 | 204.15 | 176.09 | 146.06 |
| \bar{l}_2 (nm) | 32.8 | 23.8 | 23.9 | 25.94 |
| \bar{l}_r (nm) | 26.52 | 21.3 | 21.0 | 22.0 |
| l_c (nm) | 38.78 | 39.19 | 38.45 | 35.5 |
| $2E_v/D$ (%) | 10.5 | 7.01 | 8.1 | 9.76 |
| σ | 0.03 | 0.19 | 0.02 | 0.02 |

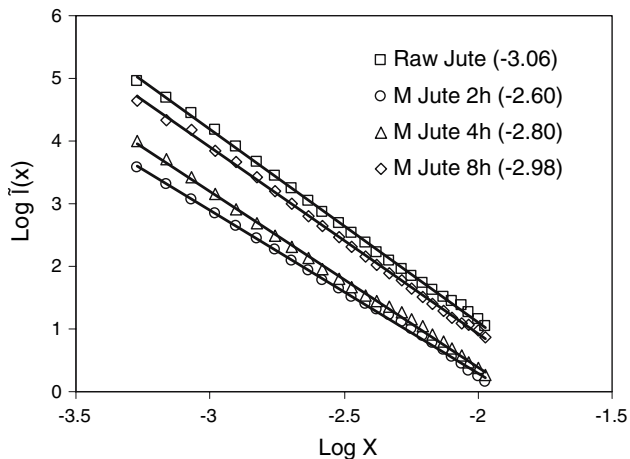


Fig. 5 Double logarithmic plot of background-corrected, smeared-out scattering curve for different jute fibres

Vonk the width of transition layer (E_v) was obtained from the plot $-(4/R(dC(r)/dr))$ versus r in Fig. 8.

The value of average periodicity transverse to the layer (D) were obtained from the position of first subsidiary maxima in one-dimensional correlation function (Fig. 7). The value of specific inner surface (S/V), the volume fraction of matter and void (ϕ_1 and ϕ_2), the transversal length in matter an void (\bar{l}_1 and \bar{l}_2), the range of inhomogeneity \bar{l}_r and the length of the coherence, \bar{l}_c were estimated. All main SAXS parameters are tabulated in Table 2. All the tabulated data are consistence with those observed for other natural fibres like cotton [40], and sisal [41].

The width of the transition layer can also be calculated using the Ruland’s method. Plot between X^{-2} vs. $\bar{I}(x) \cdot X$

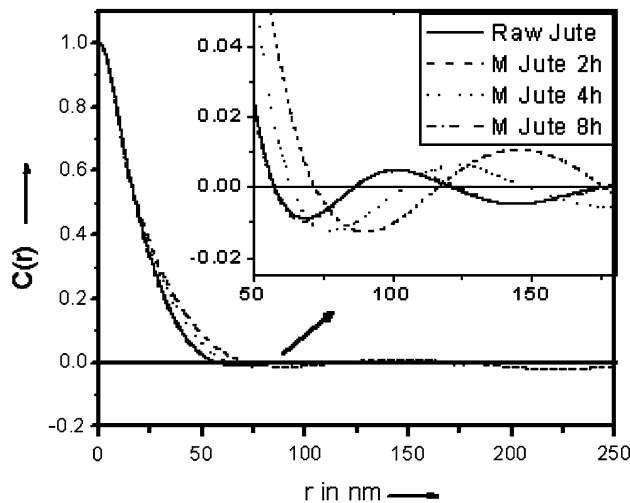


Fig. 6 The curve showing the three-dimensional correlation function $C(r)$ against r values for raw jute, M jute 2 h, M jute 4 h and M jute 8 h

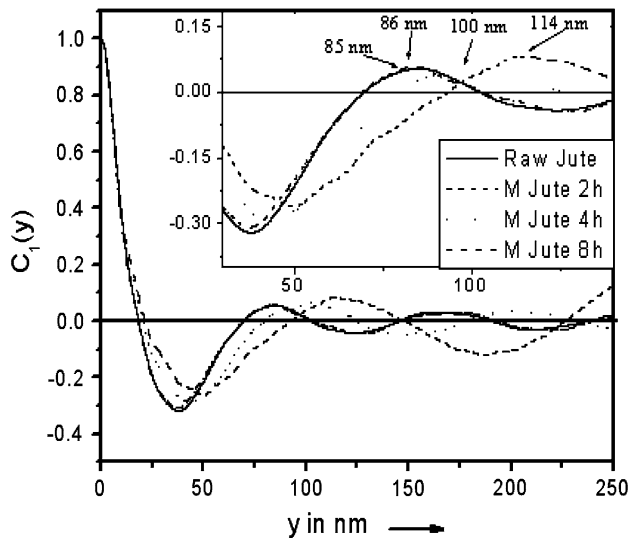


Fig. 7 The curve showing the values of one-dimensional correlation function $C_1(y)$ against y values for raw jute, M jute 2 h, M jute 4 h and M jute 8 h

is popularly known as Ruland’s plot. The Ruland’s plots were plotted taking 40 background corrected intensity values are shown in Fig. 9. Straight lines were fitted taking 15 extreme points of the tail region of the corresponding scattering curve. The negative intercept of the regression line confirms the non-ideal, two-phase system [42].

The values of E_R , the width of the transition layer, determined by Ruland method [27], were computed for each sample on substituting the values of slope (m) and y intercept (b) of the line in the relation, $E_R = \{(-6b/m)^{1/2}\} / \{2\pi/\lambda a\}$ and were tabulated in Table 2. The standard deviation of the intensities $\sigma(\sqrt{\bar{I}})$ was

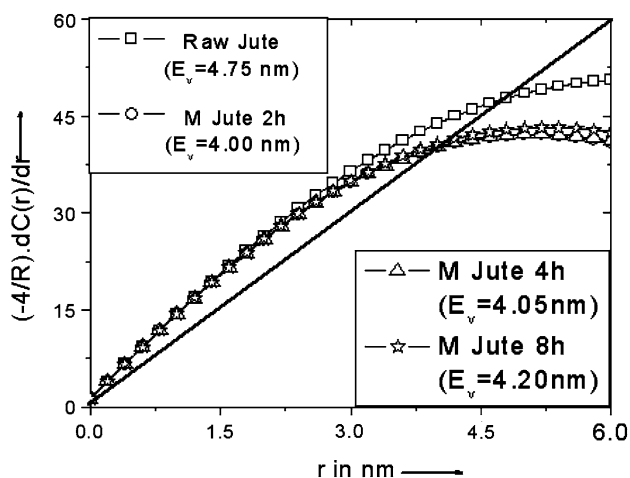


Fig. 8 The curve showing the value of $(-4/R)dC(r)/dr$ against r values for different jute fibres; the values of E_v for representative fibre are given in the parenthesis

calculated at the tail region of the SAXS curve of the samples and values are well with in permissible limits (0.5) (Table 2) [37].

Table 2 shows that the average periodicity transverse to the layer D was increased after the alkali treatment in comparison to the raw jute fibres. Similarly, the value of the volume fraction of the matter region ϕ_1 and the value of transversal length in matter phase \tilde{l}_1 were found to increase

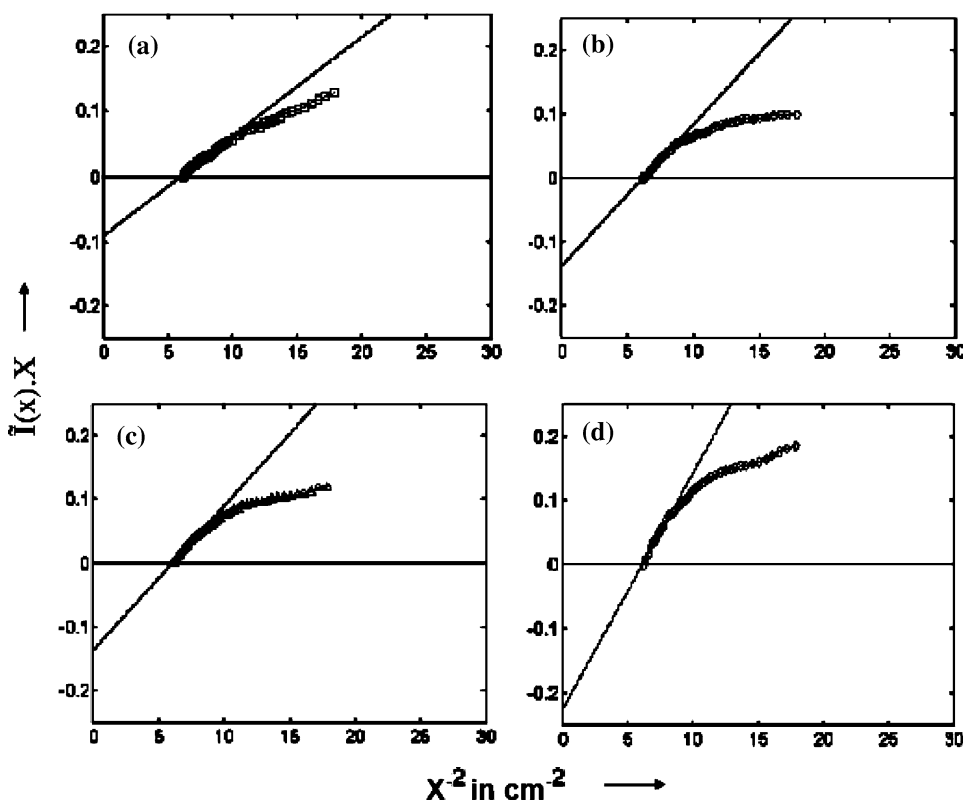
after alkali treatment. This suggests the swelling behaviour of the cellulose after the alkali treatment. It is also observed that maximum swelling was at the 2 h alkali treatment. This may be due to heavy dissolution of hemicellulose and Lignin at this particular treatment hour. The values of E , width of the transition layer, calculated by two different methods, i.e., Vonk [16] method and Ruland [27] plot method, referred as E_v and E_R , respectively, are in permissible range of deviation.

XRD analysis

Figure 10 shows the room temperature X-ray diffraction pattern of raw jute fibre samples before and after alkali treatment for 2, 4 and 8 h. The pattern shows the 002 peak is slightly shifting toward lower angle indicating the increase in d spacing. The microstress and percentage crystallinity are also calculated from the diffractogram and presented in Table 3.

From the table, it is clear that the FWHM of diffraction peak decreases after alkali treatment. The degree of crystallinity (CrI%), using the Segal empirical method found to increase after alkali treatment. Ray and co-workers also reported similar observation [31]. The extent of crystallinity formation by NaOH treatment was also determined from the improvement in the intensity of the peaks [31].

Fig. 9 Ruland plot $\tilde{l}(x) \cdot X$ vs. X^{-2} values for (a) raw jute, (b) M jute 2 h, (c) M jute 4 h and (d) M jute 8 h



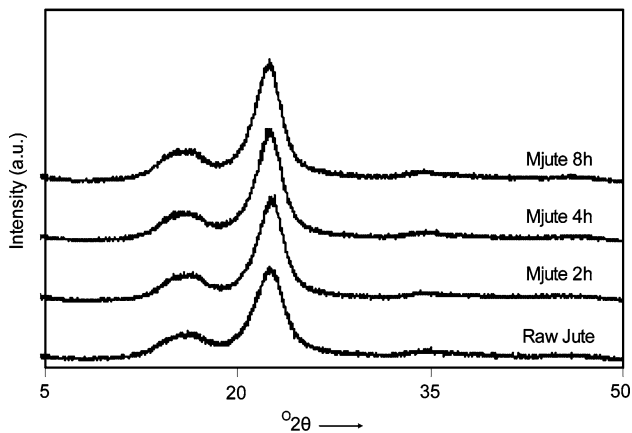


Fig. 10 X-ray diffraction pattern of jute fibre samples before and after alkali treatment

Table 3 The observed and calculated parameters from the X-ray diffraction pattern

| Parameters | Rawjute | Mjute 2 h | Mjute 4 h | Mjute 8 h |
|---|---------|-----------|-----------|-----------|
| Peak position (2θ) | 22.5 | 22.48 | 22.46 | 22.44 |
| FWHM (2θ) | 2.772 | 2.437 | 2.424 | 2.402 |
| d (nm) | 0.394 | 0.395 | 0.3954 | 0.396 |
| Crystallite size (nm) | 29 | 32 | 33 | 34 |
| ϵ | 0 | 0.002 | 0.003 | 0.004 |
| I_{002} (counts/s) | 1664 | 1836 | 1974 | 2102 |
| I_{am} (counts/s) | 569 | 554 | 585 | 615 |
| CrI (%) | 65.80 | 68.81 | 70.36 | 70.74 |
| σ_{stress} (10^{-4}) (N/tex) | 0 | 1.12 | 1.68 | 2.24 |

Mechanical properties

Figure 11 shows the variation of linear density (tex) of the fibre with alkali treatment time. The figure shows a decreasing trend of the tex with treatment time. In the present case, linear densities of the fibers decrease from 4 to 2.8, from raw jute to 8 h alkali-treated jute, respectively.

Figure 12 shows the variation of strain at break point, tenacity and modulus of the fibre with alkali treatment period. The figure shows that the modulus increased by 33% at 2 h of treatment, after which the increase was by 50% and 78% for 4 and 8 h treatments, respectively. Tenacity at break decreased after 2 h treatment, but was found to increase by nearly 22.5% after 8 h treatments. Percent (%) breaking strain was reduced by 44% after 2 h treatment, whereas the reduction was 55.5% and 72.2% after 4 and 8 h treatments, respectively. Thus, the results show that alkali-treated fibres were stiffer and brittle in comparison to raw fibres, as reported for *Corchorus capsularies* [31].

In untreated jute fibres, hemicelluloses and lignin remain dispersed in the inter-fibrillar region separating the

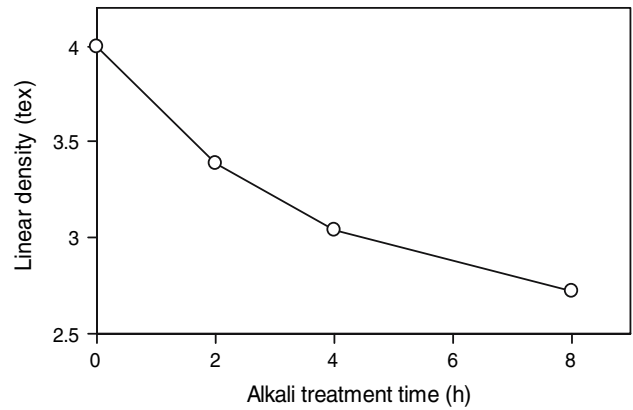


Fig. 11 The variation of linear density with alkali treatment time

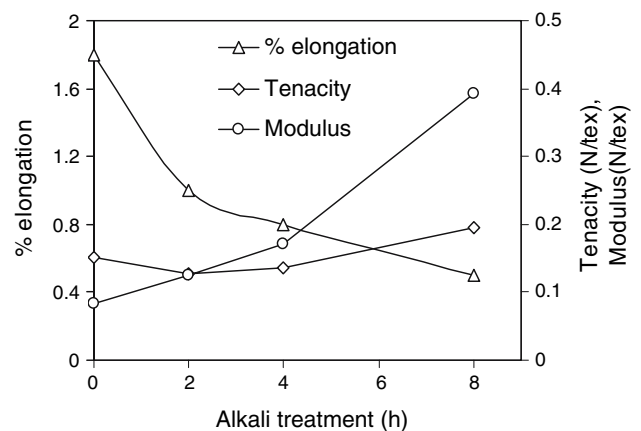


Fig. 12 The variation of strain at break point, tenacity and modulus of the fibre with alkali treatment period

cellulose chain from one another. The cellulose chains are, therefore, always in a state of constraint. Removal of hemicelluloses and lignin after alkali treatment, removed internal constraint and the fibrils became more capable of rearranging themselves in a compact manner, leading to a closer packing of the cellulose chain, which causes improvement in fibre strength and its mechanical properties. This is also responsible for the increase in the crystallinity of the fibre after alkali treatment as supported by our XRD analysis.

Thermal analysis

DSC analysis was carried out on the raw and alkali-treated jute fibres to determine the thermal behaviour of fibre. DSC analysis also enables the identification to be made of chemical activity occurring in the fibres as the temperature is increased. DSC analysis curve of raw and alkali-treated jute fibres are shown in Fig. 13. A broad endothermic peak observed in the temperature range of 60–140 °C in both

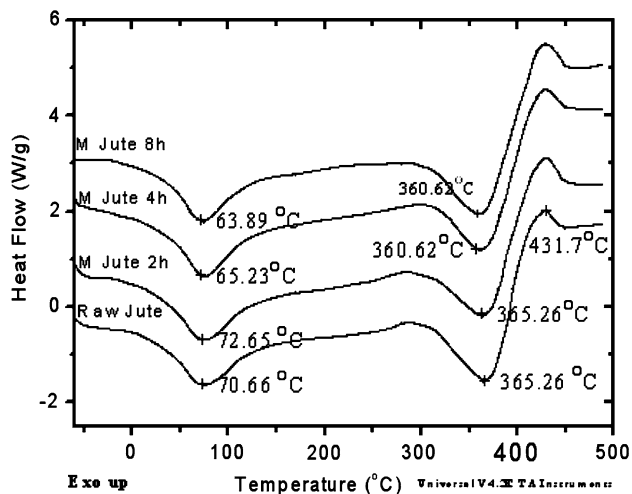


Fig. 13 DSC thermogram of raw and alkali-treated jute fibre

alkali treated and raw jute corresponds to the heat of vaporization of water absorbed in the fibres. It is reported [43] that in cellulose fibres, lignin degrades at a temperature around 200 °C while the other polysaccharides such as cellulose degrade at higher temperatures. The first exothermic hump in the DSC curve for raw jute fibre is about 290.2 °C, which is due to the thermal degradation of hemicellulose and the glycosidic linkages of cellulose. The very strong second endothermic peak at about 365.26 °C indicates the degradation of cellulose, leading to the formation of char. In addition, there is one more step with a peak at 431.7 °C. In this step, the rest of the char is oxidized and the rest of the mass consumed [44]. In the DSC curve for different alkali-treated jute fibres, it is found that the exothermic hump for decomposition of hemicellulose is very weak after 2 h alkali treatment and almost missing after 4- and 8-h alkali treatment. This may be due to the removal of hemicellulose from the fibre after alkali treatment. This is also supported by our chemical analysis plot (Fig. 1) and FT-IR spectra. According to the second endothermic peak, it can be deduced that the degradation peak of the cellulose shifted to a lower temperature, 360.62 °C from 365.26 °C after 4 and 8 h alkali treatment. This lowering of the decomposition temperature leads to the reduction in the thermal stability of alkali-treated fibres. Dipa Ray and coworkers [45] also reported the same.

Conclusion

Jute fibres (*Corchorus olitorous*) were chemically treated with 1.26 M (5 wt%) solution of NaOH for 2, 4 and 8 h. The chemical analysis of fibre and FT-IR studies revealed that hemicellulose and lignin were removed after alkali treatment and rough surface morphology of treated fibre as seen

in SEM micrograph was also due to the removal of these structural constituents. The value of periodicity transverse to the layer, D , volume fraction of the matter phase, ϕ_1 and the value of the transverse length in matter phase, \bar{l}_1 , as determined by SAXS, were found to increase after the alkali treatment. This suggests the swelling behaviour of the cellulose in the fibre due to the mercerization. Swelling is found maximum at 2 h alkali treatment. This may be due to the heavy dissolution of the hemicelluloses at this treatment time. Microstructure analysis of fibre by XRD revealed that the degree of crystallinity increased after alkali treatment. This could be due to the removal of non-crystalline structural components out of the cell wall of the fibre, leading to the closer packing of cellulose chains resulting in improved mechanical strength. But the alkali treatment led to the thermal decomposition temperature of the cellulose going down to 360.62 °C after 8 h alkali treatment from 365.26 °C for raw jute fibre, which may be due to the removal of some basic structural constituents, hemicellulose and lignin.

Acknowledgements Authors acknowledge Prof. J. Belare, IIT, Bombay, India, for providing the SAXS facility. Prof. N.V. Bhat, Emeritus Professor of Physics, Bombay Textile Research Association, is acknowledged for useful discussion and suggestion on SAXS data analysis. Prof. T.N. Tiwari, retired Professor of Physics, NIT, Rourkela, is acknowledged for thorough reading of the paper and valuable suggestion. Prof. S. Saha, NIRJAFT, Kolkata, is also acknowledged for help during the mechanical properties analysis and result interpretation.

References

- Khan F, Ahmed SR (1996) *Polym Degrad Stabil* 52:335
- Bledzki AK, Reihmane S, Gassan J (1996) *J Appl Polym Sci* 59:1329
- Gassan J, Bledzki AK (1999) *J Appl Polym Sci* 71(4):623
- Sarkar PB (1935) *Indian J Chem Soc* 12:23
- Samal RK, Mohanty M, Panda BB (1995) *J Polym Mater* 12:235
- Prasad SV, Pavithran C, Rohatgi PK (1983) *J Mater Sci* 18:1443
- Rout J, Mishra M, Nayak SK, Tripathy SS, Mohanty AK (1999) *Polymer* 99:489
- Barton HM (1950) *Phys Rev* 79:211
- Vineyard GH (1948) *Phys Rev* 74:1076
- Kratky O, Lagner P (1987) *Encycl Phys Sci Technol* 14:693
- Ratho T, Patel A (1995) *J Poly Sci Poly Chem Ed* 13(10):2345
- Mark H (1932) *Physik und chemie der zellulose*. Springer, Berlin, p 139
- Ratho T, Patel A (1981) *J Phys D Appl Phys* 14:2169; Hendricks SB (1930) *Z Kristallogr* 74:534–545 & the reference therein
- Porod G (1951) *Kolloid Z* 124:83. doi:10.1007/BF01512792
- Porod G (1952) *Kolloid Z* 125:51. doi:10.1007/BF01519615
- Vonk CG (1973) *J Appl Cryst* 6:81
- Roy AK, Bag SC, Sardar D, Sen SK (1991) *J Appl Polym Sci* 43:2187
- Roy SC (1960) *Text Res J* 30:451
- Porod G (1953) *Kolloid Z Z Polym* 133:16. doi:10.1007/BF01513900
- Ratho T, Sahu NC (1970) *Kolloid ZZ Polym* 236:43

21. Sarkar PB, Mazumdar AK, Pal KB (1948) *J Tex Inst* T44:39
22. Misra T, Patra KC, Patel T (1984) *Colloid Polym Sci* 262:611
23. Mering J, Tchoubar D (1968) *J Appl Cryst* 1:153
24. Gerber T, Walter G, Krenold R (1982) *J Appl Cryst* 15:143
25. Kortleve G, Vonk CG (1968) *Kolloid Z Z Polym* 225:124
26. Mittelbach P, Porod G (1965) *Kolloid Z Z Polym* 202:40. doi: [10.1007/BF01497184](https://doi.org/10.1007/BF01497184)
27. Ruland W (1971) *J Appl Cryst* 4:70
28. Young RJ, Bowden PB, Ritchie JM, Rider JG (1973) *J Mater Sci* 8:23
29. Cullity BD (1978) *Elements of X-ray diffraction*. Addison Wesley Publishing Company Inc, London, p 286
30. Segal L, Creely J, Martin, Conrad CM (1959) *Tex Res J* 29:786
31. Ray D, Sarkar BK, Rana AK, Bose NR (2001) *Comp Part A* 32:119
32. Gassan J, Bledzki AK (1999) *Comp Sci Tech* 59:1303
33. Khan MA, Hassan MM, Drzal LT (2005) *Comp Part A* 36:71
34. Tshboi M (1957) *J Polym Sci* 25:159
35. Liang CY, Bassett KH, Mc Ginnes EA, Marchessault RH (1960) *Tappi* 43:1917
36. Sarkar PB, Mazumdar AK (1955) *Text Res J* 12:1016
37. Vonk CG (1975) *J Appl Cryst* 8:340
38. Prasad N, Patnaik J, Bohidar N, Mishra T (1998) *J Appl Poly Sci* 67:1735
39. Mohlethaler K (1949) *Biochem Biophys Acta* 3:15
40. Misra T, Bisoyi DK, Patel T, Patra KC, Patel A (1988) *Poly J* 20:739
41. Khan MN (1995) *Small angle x-ray scattering study of sisal fibre using correlation functions*, PhD thesis, Sambalpur University, Orissa, India
42. Topping J (1972) *Error of observation and their treatment*, 4th edn. Chapman and Hall, Science paper back
43. Aziz SH, Ansell MP (2004) *Comp Sci Tech* 64:1219
44. Paunikallio T, Suvanto M, Pakkanen TT (2004) *J Appl Poly Sci* 91:2676
45. Ray D, Sarkar BK, Basak RK, Rana AK (2002) *J App Poly Sci* 85:2594